Biosensors and Bioelectronics 26 (2011) 2751–2755

Contents lists available at ScienceDirect

Biosensors and Bioelectronics

journal homepage: www.elsevier.com/locate/bios

Short communication

Monitoring the growth and drug susceptibility of individual bacteria using asynchronous magnetic bead rotation sensors

Paivo Kinnunen[a,b,1], Irene Sinn[b,c,d,1], Brandon H. McNaughton[a,b,c,*], Duane W. Newton[e,f], Mark A. Burns[d], Raoul Kopelman[a,b,c,*]

[a] The University of Michigan, Department of Chemistry, 930 N. University, Ann Arbor, MI 48109-1055, USA
[b] The University of Michigan, Applied Physics Program, 2477 Randall Laboratory, Ann Arbor, MI 48109-1120, USA
[c] The University of Michigan, Department of Biomedical Engineering, 2200 Bonisteel, Ann Arbor, MI 48109-2099, USA
[d] The University of Michigan, Department of Chemical Engineering, 2300 Hayward St., 3074 Dow, Ann Arbor, MI 48109-2136, USA
[e] The University of Michigan Health System, Clinical Microbiology and Virology Laboratories, 2F461 University Hospital, Box 5054, USA
[f] The University of Michigan Medical School, Department of Pathology, 1301 Catherine, Ann Arbor, MI 48109-0054, USA

ARTICLE INFO

Article history:
Received 23 July 2010
Received in revised form 5 October 2010
Accepted 6 October 2010
Available online 14 October 2010

Keywords:
Magnetic bead
Biosensor
Asynchronous magnetic bead rotation
Rotating magnetic field

ABSTRACT

Continuous growth of individual bacteria has been previously studied by direct observation using optical imaging. However, optical microscopy studies are inherently diffraction limited and limited in the number of individual cells that can be continuously monitored. Here we report on the use of the asynchronous magnetic bead rotation (AMBR) sensor, which is not diffraction limited. The AMBR sensor allows for the measurement of nanoscale growth dynamics of individual bacterial cells, over multiple generations. This torque-based magnetic bead sensor monitors variations in drag caused by the attachment and growth of a single bacterial cell. In this manner, we observed the growth and division of individual *Escherichia coli*, with 80-nm sensitivity to the cell length. Over the life cycle of a cell, we observed up to a 300% increase in the rotational period of the biosensor due to increased cell volume. In addition, we observed single bacterial cell growth response to antibiotics. This work demonstrates the non-microscopy limited AMBR biosensor for monitoring individual cell growth dynamics, including cell elongation, generation time, lag time, and division, as well as their sensitivity to antibiotics.

1. Introduction

Optical microscopy is currently the most widely used tool for studying single cell behavior, as it offers the ability to measure the elongation of individual bacteria over multiple generations (Brehm-Stecher and Johnson, 2004; Elfwing et al., 2004; Inoue et al., 2001). However, the spatial resolution of far-field optical microscopy techniques is limited by the diffraction of light. High sensitivity tools that have proven useful for single cell analysis include scanning probe techniques (Touhami et al., 2004) and cantilevers (Gfeller et al., 2005; Bryan et al., 2010), but studies spanning multiple generations of individual cells have not yet been demonstrated with these techniques. We note that high-resolution techniques, such as electron microscopy and cantilevers are optimal in vacuum or air, rather than in water. Here we present a high-resolution sensing method that works optimally in aqueous environments (McNaughton et al., 2007a).

In this manuscript, we implement asynchronous magnetic bead rotation (AMBR) to measure the nanogrowth of individual bacterial cells. AMBR biosensors, developed by our lab, have previously been used for a variety of applications (McNaughton et al., 2006, 2007a,b, 2009; Hecht et al., 2011; Kinnunen et al., 2010). The rotational dynamics of magnetic objects rotating asynchronously with the driving magnetic field have also been used for a other applications and studies. One of the first investigations was done on a system consisting of a ferrofluid and a pair of nonmagnetic rotating spheres called “magnetic holes” (Helgesen et al., 1990a,b). Similar magnetic rotational studies have been used for the characterization of magnetic carbon nanotubes (Korneva et al., 2005), magnetotactic bacteria (Cēbers and Ozols, 2006), traveling wave magnetophoresis (Yellen et al., 2007; Yellen and Virgin, 2009), micro mixing (Biswal and Gast, 2004; Tierno et al., 2007), and artificial microscopic swimmers and microdrills (Honda et al., 1996; Dreyfus et al., 2005). Additionally, nonmagnetic systems that undergo asynchronous rotation have been used for the rotation of glass nanorods in fluid (Shelton et al., 2005). The presented AMBR biosensor enables

* Corresponding authors at: 4744 Chemistry, 930N. University Avenue, Ann Arbor, MI 48109-1055, USA. Tel.: +1 734 764 7541; fax: +1 734 936 2778.
E-mail addresses: pkkinn@umich.edu (P. Kinnunen), isinn@umich.edu (I. Sinn), bmcnaugh@umich.edu (B.H. McNaughton), dnewton@umich.edu (D.W. Newton), maburns@umich.edu (M.A. Burns), kopelman@umich.edu (R. Kopelman).
[1] These authors contributed equally to this work.

0956-5663/$ – see front matter © 2010 Elsevier B.V. All rights reserved.
doi:10.1016/j.bios.2010.10.010

the growth of a single bacterium to be measured throughout its life cycle and over sequential generations. Indeed, we show that the elongation of individual *Escherichia coli* bacterial cells can be observed with 80 nm sensitivity in cell length. This high-sensitivity, prolonged monitoring, single cell analysis technique could be useful in population heterogeneity studies, and could radically shorten the test time for identification (ID) and antimicrobial susceptibility testing (AST) of microorganisms.

As mentioned, these single cell studies employ the AMBR biosensor, which is based on the torque exerted on a magnetic bead in the presence of a rotating magnetic field. At sufficiently high rotating field frequencies, the magnetic bead rotates asynchronously with the magnetic field, (Caroli and Pincus, 1969; Rosensweig, 1985; McNaughton et al., 2006; Cēbers and Ozols, 2006; Janssen et al., 2009) and in the case of a superparamagnetic bead the rotational period, T, is proportional to the effective volume of the rotating body, $T \propto V_{eff}$. For the derivation, see Section 2.1. Therefore, by monitoring the rotational period of the magnetic bead, it is possible to detect single bacterium binding events (McNaughton et al., 2007b) and, as demonstrated in this manuscript, measure single bacterial cell growth on the nanometer scale. When a single cell attaches to a magnetic bead, or grows, the effective volume of the bead complex increases; this process can be monitored by measuring changes in the bead's rotational period. The *E. coli* are assumed to grow only in length (Inoue et al., 2001), with a constant diameter; thus changes in the rotational period of the bead correspond to bacterial elongation. A schematic of this is shown in Fig. 1a–c. Within this manuscript, the sensitivity is defined as the smallest detectable change in the sensor or its environment.

2. Materials and methods

2.1. Theoretical derivation

The torque exerted on a magnetic bead in a magnetic field can be expressed by

$$\boldsymbol{\tau}_{mag} = \mathbf{m} \times \mathbf{B} = (\mathbf{m}_{perm} + \mathbf{m}_{ind}) \times \mathbf{B}, \tag{1}$$

where $\boldsymbol{\tau}_{mag}$ is the total magnetic torque due to the induced magnetic moment $\mathbf{m}_{ind}$ and permanent magnetic moment $\mathbf{m}_{perm}$, in a magnetic field $\mathbf{B}$. In a time varying magnetic field, the induced magnetic moment is not necessarily parallel to the magnetic field, and therefore can contribute to the torque. By using the previously described equations for asynchronous rotation, arising from magnetic torque (McNaughton et al., 2006; Cēbers and Ozols, 2006; Janssen et al., 2009), the total magnetic torque in a rotating magnetic field can be expressed by

$$\boldsymbol{\tau}_{mag} = [\mathbf{m}_{perm} + (\chi' + i\chi'')V_m\mathbf{B}] \times \boldsymbol{B} = m_{perm}B \sin(\Omega t - \theta)\hat{\mathbf{e}} + \chi'' V_m \frac{B^2}{\mu_0}\hat{\mathbf{e}}, \tag{2}$$

where χ' is the real part and χ'' is the imaginary part of the magnetic susceptibility, Ω is the driving frequency, V_m is the magnetic content volume, μ_0 the permeability of free space, and $\hat{\mathbf{e}}$ is the unit vector of the rotating field. The real part of the susceptibility, χ', does not contribute to the cross product in Eq. (2), as it remains parallel with the magnetic field. The first term on the right hand side of Eq. (2) corresponds to the permanent magnetic moment, and the second term corresponds to the induced (superparamagnetic) moment. In the experiments, we implement a 500 Hz driving field while the critical frequency of the system, Ω_c, is on the order of 1 Hz. As a result, the superparamagnetic torque dominates and the first term in Eq. (2) can be neglected ($\Omega \gg \Omega_c$). This allows for Eq. (1) to be simplified to

$$\boldsymbol{\tau}_{mag} = \mathbf{m}_{ind} \times \mathbf{B}, \tag{3}$$

leading to

$$\boldsymbol{\tau}_{mag} = \chi'' V_m \frac{B^2}{\mu_0}\hat{\mathbf{e}}. \tag{4}$$

Neglecting both inertial forces (where drag forces dominate) and Brownian rotation forces (where magnetic torque dominates) the torque of a rotating body in a viscous fluid can be expressed by:

$$\boldsymbol{\tau}_{drag} = -\boldsymbol{\tau}_{mag} = -\kappa\eta V\dot{\theta}\hat{\mathbf{e}}, \tag{5}$$

where κ is the Einstein shape factor (6 for a sphere), η is the dynamic viscosity of the surrounding fluid, V is the total volume of the rotating body, and θ is the angular orientation ($\dot{\theta}$ is the rotational rate of the object, in radians/s). The rotational rate of the object can be solved by combining Eqs. (4) and (5), which yields

$$\dot{\theta} = \frac{\chi'' V_m B^2}{\kappa\eta V\mu_0}. \tag{6}$$

At a constant temperature and a constant rotating magnetic field, the imaginary susceptibility χ'', magnetic content volume V_m, magnetic field strength B, and the dynamic viscosity η, remain constant. Under these conditions, the rotation rate of the particle is primarily a function of the effective volume

$$\dot{\theta} \propto \frac{1}{V_{eff}}. \tag{7}$$

The rotational period of the particle, T, can be written in terms of the rotational rate, $\dot{\theta}$, as $T = 2\pi/\dot{\theta}$, which yields the basis of the superparamagnetic AMBR sensor, namely Eq. (8):

$$T \propto V_{eff}. \tag{8}$$

Notably, a similar equation has been reported for the measurement of the Brownian relaxation peak of magnetic particles as measured with AC susceptometry (Astalan et al., 2004; Chung et al., 2008; Connolly and St Pierre, 2001). However, the AMBR method implements constant magnitude rotating magnetic fields and does not use varying magnitude non-rotating fields as is done with AC susceptometers. Thus, Eq. (8) does not describe the location of the Brownian relaxation peak. Instead, Eq. (8) describes how the real-time rotational period of a magnetic particle relates to the effective volume of the particle, when driven at a single frequency.

2.2. Cell culture and attachment methods

Uropathogenic *E. coli* bacteria (obtained from the Clinical Microbiology Laboratory, University of Michigan Hospital) were grown on Mueller-Hinton agar plates (BBL) at 37 °C for 12–18 h. The bacteria were then suspended in 2.2% Mueller Hinton II (MH) broth (Teknova) to the approximate concentration of 1.5×10^8 CFU/mL (e.g. a 0.5 McFarland Standard value). Anti-*E. coli* (Abcam, ab20640-1) functionalized magnetic particles (Invitrogen M-280) were introduced to the bacteria solution (to yield 10^6 beads/mL concentration). The sample was incubated, with 175 rpm shaking at 37 °C, for another 1.5 h. Before rotational data were obtained, the beads with attached bacteria were isolated using a magnetic separator (PickPen 1-M) and re-suspended into a solution containing MH broth with 1% Pluronic F-68 (King et al., 1988) (MP Biochemicals) and 0.1% BSA (Thermo Scientific). All experiments were conducted at room temperature. The ampicillin minimum inhibitory concentration (MIC) of the *E. coli* was 8 μg/mL, as determined by conventional broth microdilution methods.

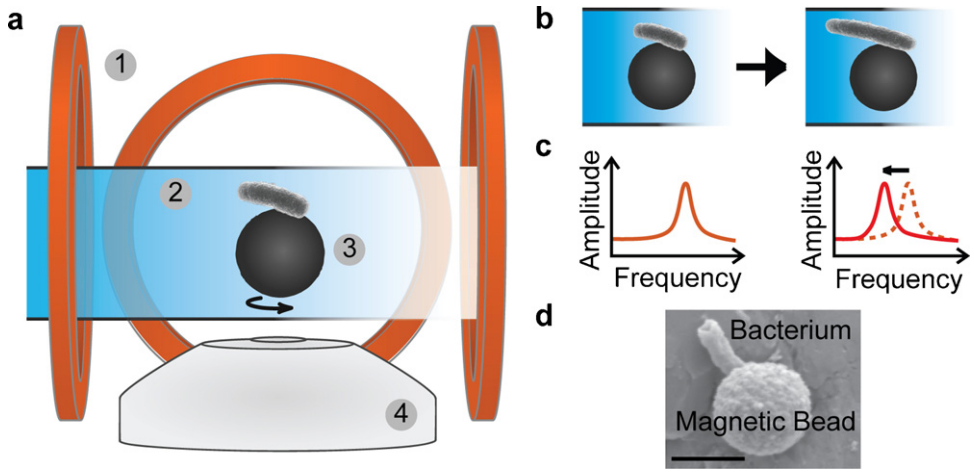

Fig. 1. The concept of measuring single cell elongation using the asynchronous magnetic bead rotation (AMBR) method. (a) A schematic representation of the AMBR sensor on a microscope, where 1. denotes the electromagnet coils, 2. the fluidic sample, 3. the AMBR biosensor with an *E. coli* attached, and 4. the microscope objective. (b) Cell elongation (schematic). (c) Schematic illustrating how the rotational period change is observed as a peak shift in the FFT spectrum (i.e. the elongation of the attached bacterium can be measured by observing the change in the rotational period of the sensor-bacterium complex, which is caused by the increase in the system's effective volume). (d) Scanning electron microscopy image of a single *E. coli* cell attached to a 2.8 μm magnetic bead. The scale bar is 2 μm.

2.3. Experimental setup and measurement conditions

Isolated bead-bacteria complexes were placed in a rotating magnetic field on an inverted optical microscope (Olympus IX71, 100×/1.3 oil) and 1 min videos were taken at 5 min intervals at 16 fps using a digital camera (Basler, piA640-210gm), see Fig. 2. Videos were analyzed using ImageJ software (Rasband, 2010) by plotting the "*z*-axis profile" of an area of interest next to the rotating particle; this yields an intensity profile that reflects the rotational frequency of the bead-bacterium complex (McNaughton et al., 2006). The intensity plot was analyzed by applying a Fast Fourier Transform (FFT) in Matlab, and the frequency of the highest amplitude FFT peak indicate the rotational rate of the particle (see Fig. 1). Occasionally, the highest amplitude FFT peak did not correspond to the observed rotational frequency of the particle, and instead was twice the observed rotational rate. The peaks were fitted with a Gaussian function in order to determine the peak position and width. The rotating magnetic field was generated with a custom Labview (National Instruments) program and Data Acquisition Board (NI PCI-6221) in conjunction with an amplifier and a custom made pair of air core Helmholtz coils. The magnetic field frequency used to rotate the magnetic beads was 500 Hz with a 0.9 mT magnitude, which was measured with a 3-axis magnetic field probe (Senis Gmbh, C-H3A-2m).

2.4. Experimental errors

The error in determining the rotational period was designated as the FFT peak width (full width at half maximum) of the amplitude signal (Figs. 2 and 3). Fixed cells (*E. coli* suspended in 1% glutaraldehyde for 30 min) were measured over 120 min, yielding a 6.0% CV in the rotational response of the sensor. Fluctuations in the rotational response of a single AMBR probe, with no bacteria present, were under 10% after 20 h, showing long-term stability in

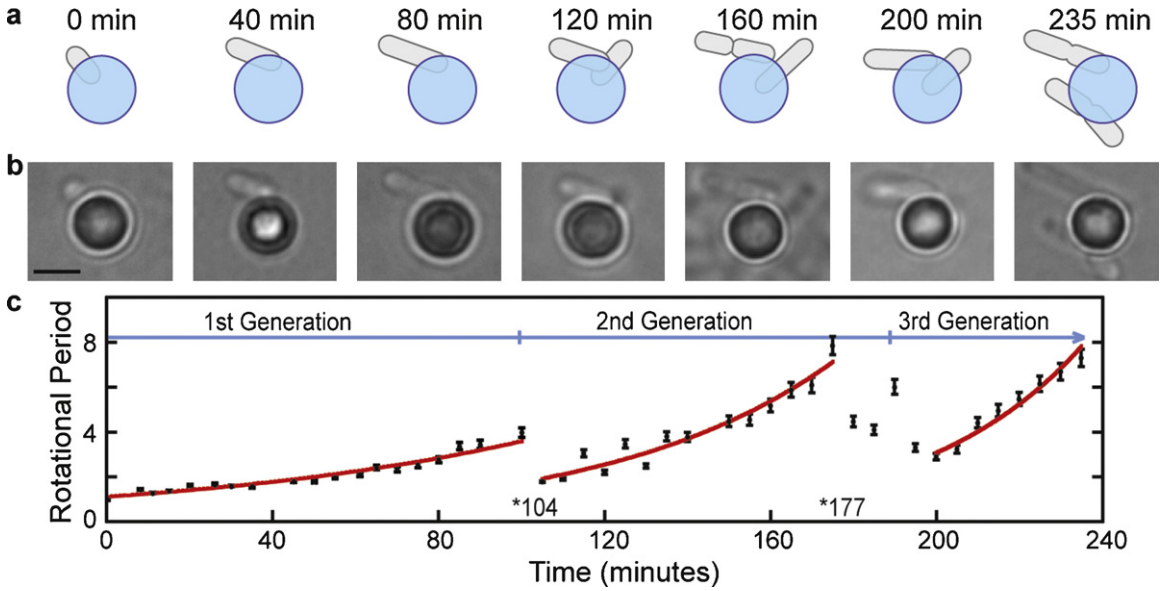

Fig. 2. Growth and division of a single *E. coli* bacterium, measured with the AMBR biosensor and observed with an optical microscope. (a) Schematic figures and (b) 100× oil immersion optical microscopy images of the AMBR sensor with initially a single bacterium attached and subsequent cell divisions. The scale bar is 2 μm (Supplementary Videos 1 and 2). (c) Cell growth and division as observed with the AMBR sensor. After a period of growth, the first cell division is observed at 104 min and again at 177 and 199 min. The error bars correspond to the measurement error in the rotational period and the exponential fits are a guide to the eye. Data is normalized to 1 at time zero.

the rotational period (data not shown). Bacterial length measurements were performed with a bright field microscope and a 100× oil immersion objective. The theoretical diffraction limit is estimated to be $\lambda/(2\text{N.A.}) \approx 700\,\text{nm}/2.6 \approx 270\,\text{nm}$, which we assumed to be our error in the bacterium length measurements on the microscope. To determine the bacterial cell length, intensity profiles were taken across the length of the bacterium, with ImageJ software.

3. Results and discussion

We demonstrated the sensitivity of the AMBR biosensor by measuring the growth and division of a single *E. coli* cell throughout its life cycle and over multiple generations (Fig. 2). Bacterial cells were attached to 2.8 μm diameter magnetic beads coated with specific antibodies. Individual cell growth and response to antibiotics were observed by using the AMBR method. Measurements were performed on an inverted bright-field microscope, which allowed for visualization of bacterial elongation and division, Fig. 2b, and quantification of the resulting changes in the rotational period of the sensor, Fig. 2c (normalized data). Over the first cell division cycle, the rotational period of the AMBR sensor changed from (0.8 ± 0.03) to (3.2 ± 0.2) s, which corresponds to a 300% increase in the rotational period. Similarly, over the second and third cell divisions, the periods changed from (1.0 ± 0.1) to (6.2 ± 0.4) s (520%) and from (2.3 ± 0.2) to (5.8 ± 0.3) s (150%), respectively. These dramatic changes in the rotational period are governed by the volumetric changes of the attached bacteria and can be seen in Supplementary Videos 1–3. The significant abrupt reduction in rotational period at time 104 min (e.g. a factor of 2.1 ± 0.3) is exactly, time wise, correlated to cell division as observed on the optical microscope. Furthermore, the rotation of the bead did not lead to the detachment of any bacteria from the bead, thus enabling studies spanning multiple generations. Detachment was only observed as a result of cell division. Upon division, the daughter cell either re-bound to the sensor or detached itself from the sensor and remained free-floating in the medium. For example, a division event that did not result in detachment can be seen in Fig. 2c at 104 min; and a division with detachment occurred at 177 min. In the case where the daughter cell remained bound to the sensor, an abrupt decrease in the rotational period was observed as the bacteria reoriented itself on the bead and lowered the effective volume (by reducing the shape factor).

Changes in the rotational period of the AMBR sensor are indeed due to bacterial growth, as there were no significant rotational period changes observed when bacteria were not present or when fixated *E. coli* cells were attached (Fig. 3a). A comparison shows that the rotational period of the AMBR sensor and the optical microscopy measurements of the cell elongation were in good agreement (Fig. 3b) and consistent with the derived linear relationship. To estimate the sensitivity of the AMBR sensor in response to cell elongation, the rotational period of the sensor was compared to the cell length as measured by optical microscopy. The sensitivity depends on the orientation of the bacterium, and is therefore case dependent. An example of the relationship between the rotational period of the AMBR sensor and the attached bacterium is shown in Fig. 3b, where the error in measuring the AMBR rotational period was estimated to correspond to (80 ± 38) nm change in bacterium length. The fit in Fig. 3b was used as the relationship between the rotational period and the bacterium length. The error in optical cell length measurements was approximately 270 nm with our microscope setup, see Section 2.4 for the calculation. We measured the rotational period from a series of images, obtained with an optical microscope; however, with the AMBR method, rotation can also be observed without a microscope, by using a combination of a low power laser and a photodiode (McNaughton et al., 2009). The authors note that the AMBR method is based on the rotational period of the magnetic particle and as a result is unaffected by the optical resolution.

To demonstrate the use of an AMBR sensor for observing single cell response to different environmental conditions, the response of individual *E. coli* cells to two concentrations of antibiotics was measured. The *E. coli* growth, in the presence of a low concentration of antibiotics (0.5 μg/mL ampicillin), and growth inhibition, in the presence of a high antibiotic concentration (8 μg/mL ampicillin), were observed using the AMBR sensor. These growth trends were again confirmed with optical microscopy (Fig. 3c). The observed response of the individual cells to the specified concentration of ampicillin should not be generalized to the whole population, since different cells within the same population may respond differently at the same concentration of antibiotics, due to the heterogeneity within the bacterial population. Nevertheless, a drastic difference is seen between the normal growth pattern below the antibiotics MIC (minimum inhibitory concentration) value and the "no growth" pattern at the MIC. The ultimate sensitivity of this method depends on the orientation of the attached bacterium and the axis of rotation of the bacterium-sensor complex. However, irrespective of this sensitivity limitation, the method can be used to clearly distinguish between growth and no growth of individual bacteria, as shown in Fig. 3c, where growth was arrested by a sufficient concentration of ampicillin. This validates the AMBR sensor as a useful tool for sensitively observing the response of individual *E. coli* cells to environmental effects, in particular to antibiotics, within only minutes.

In addition to using the AMRB sensor to study single cell response to environmental conditions, it is envisioned that this method could ultimately also be used for drug discovery research and for rapid antimicrobial susceptibility testing (AST) in clinical settings. The current clinical standard in AST is based on turbidity measurements of bacteria populations, leading to an approximately 24-h instrument time when performed on pure cultures (Jorgensen and Ferraro, 2009). Since the AMBR sensor measures the response of individual bacterial cells instead of changes in the entire population, multiplexing this technique could dramatically reduce AST

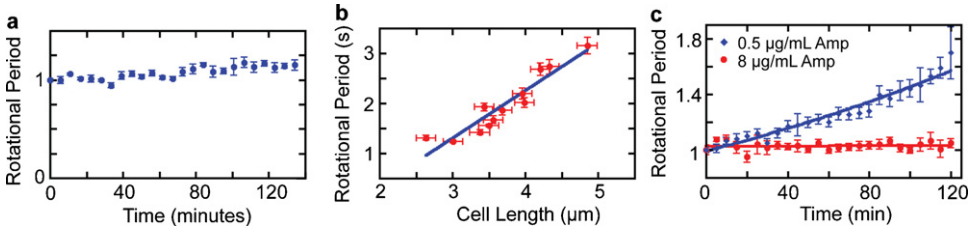

Fig. 3. AMBR sensor measurements of elongation, compared with microscope observations, and the effect of antibiotics on cell elongation. (a) Fixated *E. coli* bacterium control data; normalized rotational period of an AMBR sensor with a fixated *E. coli* attached. (b) The rotational period of the AMBR sensor vs. the bacterium length measured from microscopy images, using image analysis. The error bars in the microscope measurement data are 270 nm. The error in the rotational period of the AMBR sensor is explained in Section 2.4. (c) The response of two individual *E. coli* bacteria from the same culture (data normalized to 1 at time zero) in the presence of 0.5 and 8 μg/mL ampicillin, i.e. well below the MIC (growth) and at MIC (no growth), respectively, measured with the AMBR sensor (Supplementary Video 4).

times. Furthermore, integration with a high-throughput microfluidic technology should enable studies on growth dynamics of individual bacteria, and on their susceptibility to environmental factors such as nutrients, temperature, pH and salt levels, as well as to the introduction of antimicrobial agents.

4. Conclusions

The growth of individual *E. coli* bacteria over multiple generations and the effect of antibiotics were measured, at the nanometer scale, using the AMBR biosensor. The AMBR biosensor was observed to respond to changes of as little as 80 nm in length of single *E. coli* cells. The sensor was also demonstrated to monitor growth over the entire life cycle of the cells. Furthermore, measurement of the response of individual *E. coli* cells to 0.5 and 8 μg/mL concentrations of the antibiotic ampicillin demonstrate a drastic difference between growth and inhibition. Finally, while the demonstrated AMBR sensor has been optimized for bacteria, preliminary work has extended the method to studies on other individual cells, such as yeast and cancer cells.

Acknowledgements

We would like to thank the University of Michigan Electron Microbeam Analysis Laboratory (EMAL) for Scanning Electron Microscope access and Ron Smith for help with facilities.

Funding was provided by the National Science Foundation (DMR 0455330, RK) and the National Institute of Health (R21EB009550, RK and UL1RR024986, BHM, Postdoctoral Translational Scholar Program). BHM discloses financial interest in Life Magnetics, Inc.

Appendix A. Supplementary data

Supplementary data associated with this article can be found, in the online version, at doi:10.1016/j.bios.2010.10.010.

References

Astalan, A.P., Ahrentorp, F., Johansson, C., Larsson, K., Krozer, A., 2004. Biosensors and Bioelectronics 19, 945–951.
Biswal, S.L., Gast, A.P., 2004. Analytical Chemistry 76, 6448.
Brehm-Stecher, B.F., Johnson, E.A., 2004. Microbiology and Molecular Biology Reviews 68, 538.
Bryan, A.K., Goranov, A., Amon, A., Manalis, S.R., 2010. Proceedings of the National Academy of Sciences 107, 999.
Caroli, C., Pincus, P., 1969. Journal of Physics: Condensed Matter 9, 311–319.
Cēbers, A., Ozols, M., 2006. Physical Review E 73, 21505.
Chung, S., Grimsditch, M., Hoffmann, A., Bader, S.D., Xie, J., Peng, S., Sun, S., 2008. Journal of Magnetism and Magnetic Materials 320, 91–95.
Connolly, J., St Pierre, T.G., 2001. Journal of Magnetism and Magnetic Materials 225, 156–160.
Dreyfus, R., Baudry, J., Roper, M.L., Fermigier, M., Stone, H.A., Bibette, J., 2005. Nature 437, 862–865.
Elfwing, A., LeMarc, Y., Baranyi, J., Ballagi, A., 2004. Applied and Environmental Microbiology 70, 675.
Gfeller, K.Y., Nugaeva, N., Hegner, M., 2005. Biosensors and Bioelectronics 21 (3), 528–533.
Hecht, A., Kinnunen, P., McNaughton, B.H., Kopelman, R., 2011. Journal of Magnetism and Magnetic Materials 323, 272–278.
Helgesen, G., Pieranski, P., Skjeltorp, A.T., 1990a. Physical Review Letters 64, 1425.
Helgesen, G., Pieranski, P., Skjeltorp, A.T., 1990b. Physical Review A 42, 7271–7280.
Honda, T., Arai, K.I., Ishiyama, K., 1996. IEEE Transactions on Magnetics 32, 5085–5087.
Inoue, I., Wakamoto, Y., Moriguchi, H., Okano, K., Yasuda, K., 2001. Lab on a Chip 1, 50–55.
Janssen, X.J.A., Schellekens, A.J., van Ommering, K., van Ijzendoorn, L.J., Prins, M.W.J., 2009. Biosensors and Bioelectronics 24, 1937–1941.
Jorgensen, J.H., Ferraro, M.J., 2009. Clinical Infectious Diseases 49, 1749–1755.
King, A.T., Lowe, K.C., Mulligan, B.J., 1988. Biotechnology Letters 10, 177–180.
Kinnunen, P., Sinn, I., McNaughton, B.H., Kopelman, R., 2010. Applied Physics Letters.
Korneva, G., Ye, H., Gogotsi, Y., Halverson, D., Friedman, G., Bradley, J.C., Kornev, K.G., 2005. Nano Letters 5, 879–884.
McNaughton, B.H., Agayan, R.R., Wang, J.X., Kopelman, R., 2007a. Sensors & Actuators B: Chemical 121, 330–340.
McNaughton, B.H., Agayan, R.R., Clarke, R., Smith, R.G., Kopelman, R., 2007b. Applied Physics Letters 91, 224105.
McNaughton, B.H., Kehbein, K.A., Anker, J.N., Kopelman, R., 2006. Journal of Physical Chemistry B 110, 18958.
McNaughton, B.H., Kinnunen, P., Smith, R.G., Pei, S.N., Torres-Isea, R., Kopelman, R., Clarke, R., 2009. Journal of Magnetism and Magnetic Materials 321, 1648–1652.
Rasband, W.S., 2010. Image J.1.42q. National Institutes of Health, Bethesda, Maryland, USA.
Rosensweig, R.E., 1985. Ferrohydrodynamics. Cambridge University Press, Cambridge.
Shelton, W.A., Bonin, K.D., Walker, T.G., 2005. Physical Review E 71, 36204.
Tierno, P., Johansen, T.H., Fischer, T.M., 2007. Journal of Physical Chemistry B 111, 3077.
Touhami, A., Jericho, M.H., Beveridge, T.J., 2004. Journal of Bacteriology 186, 3286.
Yellen, B.B., Erb, R.M., Son, H.S., Hewlin, R., Shang, H., Lee, G.U., 2007. Lab on a Chip 7, 1681–1688.
Yellen, B.B., Virgin, L.N., 2009. Physical Review E 80, 011402.